KIFC1 regulates ZWINT to promote tumor progression and spheroid formation in colorectal cancer

Running title: Role of KIFC1 and ZWINT in CRC

Shintaro Akabane[1,2], Naohide Oue[1], Yohei Sekino[3], Ryuichi Asai[4], Pham Quoc Thang[1], Daiki Taniyama[1], Kazuhiro Sentani[1], Masashi Yukawa[5], Takashi Toda[5], Ken-ichi Kimura[6], Hiroyuki Egi[2], Wataru Shimizu[2], Hideki Ohdan[2], Wataru Yasui[1*]

[1] Department of Molecular Pathology, Graduate School of Biomedical and Health Sciences, Hiroshima University

[2] Department of Gastroenterological and Transplant Surgery, Graduate School of Biomedical and Health Sciences, Hiroshima University

[3] Department of Urology, Graduate School of Biomedical and Health Sciences, Hiroshima University

[4] Department of Surgical Oncology, Graduate School of Medicine, Gifu University

[5] Hiroshima Research Center for Healthy Aging, Department of Molecular Biotechnology, Graduate School of Integrated Sciences for Life, Hiroshima University

[6] Chemical Biology Laboratory, Graduate School of Arts and Sciences, Iwate University

***Corresponding author:**

Wataru Yasui, MD, PhD

Department of Molecular Pathology, Graduate School of Biomedical and Health Sciences, Hiroshima University, 1-2-3, Kasumi, Minami-ku, Hiroshima 734-8551, Japan.

E-mail address: wyasui@hiroshima-u.ac.jp

Phone number: +81 82 257 5145, Fax number: +81 82 257 5149

Abbreviated words:

ALDH1, aldehyde dehydrogenase 1; CI, confidence interval; CRC, colorectal cancer; CSCs, cancer stem cells; EGFR, epidermal growth factor receptor; KIFC1, kinesin family member C1; MTT, 3-(4,5-dimethylthiazol-2-yl)-2,5-diphenyltetrazolium bromide; KAA, kolavenic acid analog; siRNA, small interfering RNA; TCGA, The Cancer Genome Atlas; ZWINT, ZW10 interacting kinetochore protein

ABSTRACT

Colorectal cancer (CRC) is the second leading cause of cancer-related mortality worldwide. Kinesin Family Member C1 (KIFC1) has been proposed as a promising therapeutic target due to its pivotal role in centrosome clustering to mediate cancer cell progression. This study aimed to analyze the expression and biological function of KIFC1 in CRC. Immunohistochemically, 67 (52%) of 129 CRC cases were positive for KIFC1 and statistically associated with poorer overall survival. KIFC1 siRNA-transfected cells demonstrated lower cell proliferation as compared to the negative control cells. A specific KIFC1 inhibitor, kolavenic acid analog (KAA) drastically inhibited CRC cell proliferation. Microarray analysis revealed that KAA-treated CRC cells presented reduced ZW10 interacting kinetochore protein (ZWINT) expression as compared to control cells. Immunohistochemical analysis demonstrated that 61 (47%) of 129 CRC cases were positive for ZWINT and ZWINT expression was significantly correlated with KIFC1 expression. ZWINT-positive cases exhibited significantly worse overall survival. KIFC1 siRNA-transfected cells showed reduced ZWINT expression while ZWINT siRNA-transfected cells decreased cell proliferation. Both KIFC1 and ZWINT knockdown cells attenuated spheroid formation ability. This study provides new insights into KIFC1 regulating ZWINT in CRC progression and its potential as a therapeutic target.

Keywords: colorectal cancer, KIFC1, kolavenic acid analog, ZWINT

Introduction

Colorectal cancer (CRC) is estimated to have more than 1.8 million new cases (ranks third) and 881,000 deaths (ranks second) worldwide according to the Global Cancer Statistics in 2018.[1] The survival rate of patients with early-stage CRC is relatively high; however, approximately 60 % of the cases are found in the later stage.[2] The five-year survival rate of stage IV patients is estimated to drop as low as 12.5 %.[3] Therefore, there is an urgent need for determining a novel molecular target for CRC treatment strategies.

In recent years, cancer has been regarded as a stem cell disease.[4] In solid tumors, cancer stem cells (CSCs) have been characterized by specific cell surface markers, such as CD44, CD133, and aldehyde dehydrogenase 1 (ALDH1).[5] Generally, in the process of spheroid colony formation, cells are cultured in non-attachment dishes with serum-free media, which effectively enriches CSCs.[6] Previously, we examined the gene expression profile of the spheroid colonies formed by gastric cancer (GC) cells using microarray analysis and found that kinesin family member C1 (*KIFC1*) expression was upregulated in GC spheroid colonies.[7] The kinesin superfamily proteins share a motor domain and participate in several biological functions.[8] Reportedly, KIFC1 plays a pivotal role in centrosome clustering in cancer cells and is related to the pathogenesis of several cancer types.[9–11] Generally, cancer cells with centrosome amplification lead to apoptosis through multipolar mitosis; however, centrosome clustering could prevent cell death causing the formation of pseudo-bipolar structures.[12] Although in our previous

study, we reported that KIFC1 is overexpressed in gastric, esophageal, and prostate cancers and this overexpression is probably involved in cancer stemness,[7,13,14] the role of KIFC1 in CRC is yet to be investigated. Therefore, we aimed to investigate KIFC1 expression using immunohistochemistry, examine the association between KIFC1 expression and clinicopathologic characteristics, and analyze the biological function of KIFC1 with small interfering RNA (siRNA) on cell growth and spheroid formation in CRC cells in the present study.

Previously, kolavenic acid analog (KAA), a natural compound, has been identified as a KIFC1-specific inhibitor through the screening method using KIFC1-overproducing fission yeast cells.[15,16] In the current study, we aimed to elucidate the effect of this compound on CRC cell proliferation. Further, we conducted microarray analysis to reveal the change in expression of several genes, including *KIFC1*, investigated the level of ZW10 interacting kinetochore protein (*ZWINT*) expression and elucidated the biological role of ZWINT in CRC.

Materials and methods

Tissue samples and cell lines

In a retrospective study design, 129 surgically resected tumors were collected from CRC patients underwent curative resection between 2006 and 2010 at Hiroshima

University Hospital (Hiroshima, Japan). Because written informed consent was not obtained, for strict privacy protection, all of the identifying information associated with the samples was removed before the analysis. This study was approved by the Ethical Committee for Human Genome Research of Hiroshima University, Hiroshima, Japan (no. IRINHI66). We previously demonstrated that KIFC1 induces resistance to chemotherapy,[14] we considered the preoperative treatment could affect the expression status of KIFC1. Therefore, patients who received preoperative radiotherapy or chemotherapy were excluded from the study. Further, operative mortality was defined as death within 30 days of patients leaving the hospital, wherein these patients were also excluded from the analysis. Postoperative follow-up appointments were scheduled every 3 months during the first 2 years and every 6 months over the next 3 years and yearly thereafter. Chest X-ray, computed tomography scan, and serum tumor markers were assessed at every follow-up visit. Patients were followed by their respective physicians until the patients' death or the date of the last documented contact. Human colon cancer-derived cell lines, DLD-1, LoVo, WiDr, and COLO201 were purchased from the Japanese Collection of Research Bioresources Cell Bank (Osaka, Japan). All cell lines were maintained in RPMI-1640 medium (Nissui Pharmaceutical Co., Ltd., Tokyo, Japan) containing 10 % fetal bovine serum (BioWhittaker, Walkersville, MD, USA) in a humidified atmosphere of 5 % CO_2 and 95 % air at 37 ˚C.

Immunohistochemistry

One or two representative tumor blocks, including the tumor center, invasive front, and tumor-associated non-neoplastic mucosa, were examined from each sample by immunohistochemistry. In case of large, late-stage tumors, two different sections were examined to include representative areas of the tumor center as well as of the lateral and deep tumor invasive front. Immunohistochemical analysis was performed using Dako EnVision+ Mouse Peroxidase Detection System (Dako Cytomation, Carpinteria, CA, USA). Antigen retrieval was performed by microwave heating in citrate buffer (pH 6.0) for 30 min. Peroxidase activity was blocked with 3 % H_2O_2-methanol for 10 min and non-specific antibody binding sites were blocked by incubating the sections with normal goat serum (Dako Cytomation) for 20 min. Further, the sections were incubated with mouse monoclonal anti-KIFC1 (1:100; Abnova), anti-CD44 (1:100, clone DF1485; Novocastra), anti-ALDH1 (1:400, clone 44/ALDH1; BD Biosciences), and rabbit polyclonal anti-ZWINT (1:50, clone HPA005757; Sigma-Aldrich) antibodies for 1 h at room temperature, followed by incubation with EnVision+ anti-mouse peroxidase for 1 h. For color reaction, sections were incubated with the DAB substrate-chromogen solution (Dako Cytomation) for 10 min. Sections were counterstained with 0.1 % hematoxylin. Negative controls were created by the omission of the primary antibody. Expressions of KIFC1, CD44, and ALDH1 were evaluated as positive when >10 % of tumor cells were stained. ZWINT immunostaining was evaluated and scored using German immunoreactive score as previously described.[18] Intensity score was assessed as 0 (negative), 1 (weak), 2 (moderate), and 3 (strong). Percentage of positive tumor cells were scored as 0 (< 5 %), 1 (5 %–25 %), 2 (25 %–50 %), 3 (50 %–75 %), or 4 (>

75 %). Staining intensity and staining area scores were multiplied as the final immunoreactive score of ZWINT expression. Subsequently, a final score ≥ 6 was defined as ZWINT-positive and a score ≤ 4 was defined as ZWINT-negative. Using these definitions, two surgical pathologists (NO and KS), without knowledge of the clinicopathological parameters or the patients' outcomes, independently reviewed immunoreactivity in each specimen. Interobserver differences were resolved by consensus review at a double-headed microscope after independent review.

RNAi and cell growth assay

siRNA oligonucleotides targeting KIFC1, ZWINT, and negative control were purchased from Invitrogen (Carlsbad, CA, USA). We used two independent KIFC1 and ZWINT siRNA oligonucleotide sequences. Transfection was performed using Lipofectamine RNAiMAX (Invitrogen) as previously described.[20] Briefly, 60 pmol of siRNA and 10 μL of Lipofectamine RNAiMAX were mixed in 1 mL of RPMI-1640 medium (10 nmol/L final siRNA concentration). After 20 min of incubation, the mixture was added to cells, and then cells were plated in culture dishes. Forty-eight hours after transfection, cells were analyzed as described further. To examine cell growth, MTT [3-(4,5-dimethylthiazol-2-yl)-2,5-diphenyltetrazolium bromide] assay was performed. The transfected cells were seeded at a density of 4,000 cells/well in 96-well plates. Cell growth was monitored at 1, 2, and 4 days.

Spheroid colony formation

For the generation of spheroids, 1,000 cells were seeded in a 6-well ultra-low attachment plate (Corning, Corning, NY, USA). Cells were grown in mTeSR medium (StemCell Technologies Inc.). The plates were incubated at 37 °C in an incubator with a 5 % CO_2 atmosphere for 15 days. Spheroid number and size were determined and counted under a microscope.

Treatment by KIFC1 inhibitor, and gene expression analysis

Kolavenic acid analog (KAA) was previously isolated from *Solidago altissima* and identified as a KIFC1-specific inhibitor.[15,16] It was dissolved in DMSO as a stock solution and stored at -20℃ before use. DLD-1 and WiDr cells were treated with KAA followed by MTT assays performed at 1, 2, and 4 days. Further, microarray analysis was performed using the Affymetrix GeneChip® manual (Affymetrix Inc., Santa Clara, CA, USA), as previously described.[21] RNA was isolated from DLD-1 cells treated with KAA (25 μM) for 48 h and control cells. Gene alteration was calculated by fold change.

Statistical methods

Associations between clinicopathological parameters and KIFC1 (ZWINT) expression were analyzed by Fisher's exact test. We used Kaplan–Meier method to assess survival estimates and log-rank test to compare KIFC1 (ZWINT)-positive and negative cases.

The association between clinical covariates and cancer-specific mortality was evaluated using univariate and multivariate Cox regression analyses. Hazard ratio (HR) with its 95 % confidence interval (CI) was estimated accordingly. Differences between groups in the MTT and spheroid formation assays were evaluated by the Student t-test. Cell growth and spheroid formation assays involved three independent experiments; mean ± SD was calculated for each of these experiments. SPSS, ver. 24 (IBM Corp, Armonk, NY, USA) was used for these analyses, with a significant level set at $p < 0.05$.

Quantitative reverse transcription PCR (qRT-PCR), Western blot, Gene expression data from The Cancer Genome Atlas (TCGA), Wound healing assay, Conventional adenoma tissue samples

These methods are described in detail in the Supporting Information.

Results

Expression of KIFC1 in CRC tissue samples

We first investigated the *KIFC1* mRNA expression in 14 types of normal tissue and 28 CRC tissue samples by qRT-PCR. Clinicopathologic characteristics of these 28 CRC tissue samples are shown in Supporting Table 2. The gastrointestinal tissues (stomach,

small intestine, and colon) showed a relatively high *KIFC1* expression among the normal tissue samples, whereas the CRC tissue samples showed remarkably higher *KIFC1* expression as compared to the normal colon tissue. (Fig. 1a). We next performed immunohistochemical analysis in 129 surgically resected CRC tissue samples. Weak or no staining of KIFC1 was observed in the epithelial and stromal cells of non-neoplastic colonic mucosa. Conversely, CRC tissue samples showed robust, more extensive staining mainly in the nucleus (Fig. 1b). Many CRC tissue samples demonstrated heterogeneous KIFC1 staining wherein the proportion of KIFC1-stained CRC cells ranged from 0 % to 40 %. Upregulation of KIFC1 in the invasive front was not found. We regarded KIFC1 immunostaining as positive when more than 10 % of the tumor cells were stained. In total, 67 (52 %) of 129 CRC cases were found positive for KIFC1. We further investigated the relationship between KIFC1 and CSC markers by immunohistochemistry and found that CD44 and ALDH1 were mainly stained in the membrane and the cytoplasm of the CRC cells, respectively (Fig. 1c). KIFC1-positive CRC cases were significantly correlated with CD44-positive ($p = 0.011$) and ALDH1-positive ($p = 0.009$) cases (Table 1). We then examined the relationship between KIFC1 expression and clinicopathological characteristics (Table 2). KIFC1-positive cases were significantly associated with N and M stages and showed significantly poorer overall survival (Fig. 1d). In TCGA database, short-term survival (1 to 80 months) in CRC patients with high *KIFC1* expression was significantly decreased as compared to those with low *KIFC1* expression (Fig. 1e), which was consistent with our analysis. Further, multivariate analysis showed that KIFC1 expression was an independent prognostic

factor for overall survival in CRC patients (Table 3). These results indicate that KIFC1 expression is associated with CRC progression and could be involved in CRC stemness.

KIFC1 inhibition affected cell growth, EGFR-related pathway, and spheroid formation in CRC cells

We next examined the biological role of KIFC1 using CRC cell lines. Western blot analysis revealed various levels of KIFC1 expression in CRC cells (Fig. 2a). We selected DLD-1 and WiDr cells that showed high KIFC1 expression for further experiments. We found that the KIFC1 expression was substantially suppressed by treatment with KIFC1-specific siRNAs (siRNA1 and siRNA2) by immunoblotting (Fig. 2b). MTT assays performed after siRNA transfection demonstrated that KIFC1 siRNA-transfected cells showed significantly reduced cell growth as compared to the negative control cells (Fig. 2c). It has been reported that epidermal growth factor receptor (EGFR) activates the Ras-mitogen-activated protein kinase kinase-Erk and Akt-phosphatidylinositol- 4,5-bisphosphate 3-kinase signaling pathways which lead to cancer cell proliferation and survival in colorectal cancer.[22,23] To investigate the KIFC1-induced activation of EGFR-related pathway in CRC, we analyzed the levels of Akt and Erk phosphorylation in CRC cells with KIFC1 inhibition. Consequently, we found that the levels of phosphorylated Akt and Erk (pAkt and pErk, respectively) were reduced in KIFC1 siRNA-transfected cells (Fig. 2b). We next analyzed the association between KIFC1 expression and spheroid formation ability in CRC cells. We observed that the

number and size of spheroids were significantly reduced in KIFC1 siRNA-transfected cells as compared to the control cells (Fig. 2d). These results suggest that KIFC1 is involved in cell growth through the EGFR-related pathway and is required for spheroid formation in CRC.

KIFC1-specific inhibitor blocked cell proliferation and altered gene expression

DLD-1 and WiDr cells were treated with KAA at various concentrations for 4 days. MTT assays showed that KAA inhibited cell proliferation in a dose-dependent manner (Fig. 3a). Wound healing assay also revealed that KAA inhibited CRC migration in a dose-dependent manner (Supporting Figure 1). Microarray analysis to evaluate the gene alterations by KAA revealed multiple genes that were significantly decreased by KIFC1 inhibition (Supporting Table 3). We examined the expressions of these genes in 10 CRC tissue samples and calculated the ratio of mRNA expression levels between cancer tissue (T) and corresponding non-neoplastic mucosa (N). From a total of seven genes, *ZWINT* was overexpressed (T/N ratio of > 2) in 6 (60 %) of the 10 cases (Supporting Figure 2). Therefore, we next investigated the expression of ZWINT in CRC. Immunohistochemical analysis showed that ZWINT expression was observed mainly in the cytoplasm of cancer cells and KIFC1-positive regions (Fig. 3b). In total, 61 (47 %) of 129 CRC cases were positive for ZWINT. Moreover, ZWINT-positive cases were significantly associated with KIFC1-positive cases (Table 2) and higher TNM stages (Supporting Table 4). We additionally investigated the expressions of KIFC1 and

ZWINT in colorectal adenoma specimens and found that these molecules were scarcely detected (images are not shown), suggesting that KIFC1 and ZWINT would not be involved in the conventional adenoma-carcinoma pathway (Supporting Figure 3). ZWINT-positive cases showed poorer overall survival (Fig. 3c), whereas the short-term survival of CRC patients with high *ZWINT* expression was not statistically significant in TCGA database (data not shown). We further analyzed the expressions of these genes using TCGA database (n = 512) and found that *ZWINT* expression was significantly correlated with *KIFC1* expression (Fig. 3d). Further, multivariate analysis showed that ZWINT expression was an independent prognostic factor for overall survival (Table 3). We next confirmed the protein reduction in CRC cells after KAA treatment (25 μM) and found that KIFC1 and ZWINT were downregulated in a time-dependent manner (Fig. 3e). We also demonstrated that the expression of ZWINT was reduced in KIFC1 siRNA-transfected cells (Fig. 3f). These results indicate that the KIFC1 inhibitor could block CRC cell proliferation and regulate ZWINT expression that affects the prognosis of CRC.

ZWINT inhibition affected cell growth, EGFR-related pathway, and spheroid formation

We next investigated the effect of ZWINT inhibition on CRC cell functions. We confirmed reduced expression of ZWINT by the transfection of ZWINT-specific siRNAs (siRNA1 and siRNA2) (Fig. 4a). MTT assay showed decreased cell growth

ability in ZWINT siRNA-transfected cells (Fig. 4b). Levels of pAkt and pErk were reduced in ZWINT siRNA-transfected cells as compared to the negative control cells, whereas the expression of KFC1 was not affected by ZWINT knockdown (Fig. 4a). Further, the number and the size of spheroids of ZWINT siRNA-transfected cells were significantly smaller than those of the negative control cells (Fig. 4c). These results indicate that *ZWINT* could play a crucial role as a downstream gene of *KIFC1* in CRC progression.

Discussion

In the present study, we found a novel association between KIFC1 and CRC. We demonstrated that 52 % of our study cohort were positive for KIFC1 in the immunohistochemical analysis and KIFC1 expression was significantly associated with later-stage disease and poorer prognosis. In the current situation, the survival of CRC patients with the metastatic disease still remains low in spite of the development of chemotherapies.[24] Further, lymph node-positive CRC patients who receive conventional oxaliplatin-based adjuvant chemotherapy suffer from severe sensory neurotoxicity.[25] KIFC1 plays an important role in centrosome clustering for cancer cell survival,[12,26] whereas KIFC1 is dispensable in normal cells that have only one pair of centrosomes.[27] Both the qRT-PCR and immunohistochemical analyses presented that the expression of KIFC1 in CRC tissue samples was much higher than that of the normal tissue samples.

We further demonstrated that KAA (KIFC1-specific inhibitor) could drastically inhibit CRC cell proliferation and migration. These results indicate that KIFC1-inhibiting strategy would entail an aggressive effect on CRC with fewer adverse events and that immunohistochemical analysis of KIFC1 could be available in selecting patients who benefit from KIFC1-targeted therapy.

Microarray analysis demonstrated that *ZWINT* was downregulated in KAA-treated cells. ZWINT is previously identified as an essential component of chromosome motility and spindle checkpoint control.[28,29] ZWINT overexpression has been associated with poor prognosis in hepatocellular carcinoma and lung cancer,[18,30] whereas the expression and biological role of ZWINT in CRC has not been investigated. In our immunohistochemical analysis, we found that the positivities between KIFC1 and ZWINT were significantly correlated and both expressions were independent prognostic predictors in CRC patients. In the cell functional analysis, KIFC1 and ZWINT inhibition significantly reduced cell proliferation. We further confirmed that the expressions of pAkt and pErk were suppressed by KIFC1 and ZWINT knockdown, indicating that these genes might be involved in the activation of the EGFR-related pathway in CRC progression. Taken together, these results suggest that KIFC1 and ZWINT could be involved in the malignant behavior of CRC.

CSC-targeting strategies are of great importance because CSCs are associated with several malignant features of CRC.[31] We previously demonstrated that KIFC1 could affect cancer stemness.[7,13,14] In this study, we showed that KIFC1-positive cases showed a significant correlation with CD44 and ALDH1-positive CRC cases. CSCs have been

reported to be a minor population (< 5 %) of cancer cells;[32] however, immunohistochemical analysis showed the various proportions of KIFC1-stained CRC cells, which ranged from 0 % to 40 %, implying that KIFC1 would not be a specific marker for colorectal CSCs. We also found that KIFC1 and ZWINT knockdown further reduced the spheroid formation ability of CRC cells, indicating that these genes could be involved in CRC stemness. Reportedly, *KIFC1* and *ZWINT* are key genes associated with cancer stemness in other cancer types as demonstrated by in silico analyses.[33,34] however, the underlying mechanism between CRC stemness and these genes remain unknown. Further investigation is warranted to clarify the biological implications of KIFC1 and ZWINT in colorectal CSCs.

There are certain limitations associated with this study. Firstly, this study was a retrospective one involving a small size of clinical samples for the immunohistochemical analyses. A prospective study with a larger number of CRC patients is needed to verify our study findings. Secondly, the mechanism of direct or indirect interaction between KIFC1 and ZWINT is still unclear that demands further analysis in this regard.

In summary, this study demonstrated that KIFC1 regulated ZWINT to facilitate CRC progression and could induce an unfavorable prognosis among CRC patients. Further, in vitro experiments showed that KIFC1 and ZWINT affected cell proliferation via EGFR-related pathway and spheroid formation. We found that the KIFC1 inhibitor dramatically reduced CRC cell proliferation, indicating that KIFC1 could be a promising therapeutic target for CRC.

Acknowledgments

The authors are grateful to Mr. Shinichi Norimura for his excellent technical assistance and advice. This work was supported by Grants-in-Aid for Scientific Research and for Challenging Exploratory Research from the Japan Society for the Promotion of Science and the Takeda Science Foundation.

Disclosure statement

None declared.

Author Contributions

SA (first author), NO and WS (corresponding author) conceptualized and designed the study. SA performed data collection and analyses. YS, RA, PQT, DT, and KS assisted the molecular technologies used. MY, TT and KK isolated the chemical substance used in the experiment. HE, WS, and HO performed the surgical care and provided clinical samples. SA drafted the manuscript. NO provided inputs regarding manuscript preparation. WS contributed to manuscript preparation. All authors have read and approved the final manuscript.

References

1. Bray F, Ferlay J, Soerjomataram I, Siegel RL, Torre LA, Jemal A. Global cancer statistics 2018: GLOBOCAN estimates of incidence and mortality worldwide for 36 cancers in 185 countries. *CA Cancer J Clin*. 2018; **68**: 394-424.

2. Favoriti P, Carbone G, Greco M, Pirozzi F, Pirozzi REM, Corcione F. Worldwide burden of colorectal cancer: a review. *Updates Surg*. 2016; **68**: 7-11.

3. DeSantis CE, Lin CC, Mariotto AB, et al. Cancer treatment and survivorship statistics, 2014. *CA Cancer J Clin*. 2014; **64**: 252-71.

4. Bessède E, Dubus P, Mégraud F, Varon C. Helicobacter pylori infection and stem cells at the origin of gastric cancer. *Oncogene*. 2015; **34**: 2547-55.

5. Wakamatsu Y, Sakamoto N, Oo HZ, et al. Expression of cancer stem cell markers ALDH1, CD44 and CD133 in primary tumor and lymph node metastasis of gastric cancer. *Pathol Int*. 2012; **62**: 112-9.

6. Takaishi S, Okumura T, Wang TC. Gastric cancer stem cells. *J Clin Oncol*. 2008; **26**: 2876-82.

7. Oue N, Mukai S, Imai T, et al. Induction of KIFC1 expression in gastric cancer spheroids. *Oncol Rep*. 2016; **36**: 349-55.

8. Liu X, Gong H, Huang K. Oncogenic role of kinesin proteins and targeting kinesin therapy. *Cancer Sci*. 2013; **104**: 651-56.

9. Pannu V, Rida PCG, Ogden A, et al. HSET overexpression fuels tumor progression via centrosome clustering-independent mechanisms in breast cancer patients. *Oncotarget*. 2015; **6**: 6076-91.

10. Han J, Wang F, Lan Y, et al. KIFC1 regulated by miR-532-3p promotes epithelial-to-mesenchymal transition and metastasis of hepatocellular carcinoma via gankyrin/AKT signaling. *Oncogene*. 2019; **38**: 406-20.

11. Li G, Chong T, Yang J, Li H, Chen H. Kinesin motor protein KIFC1 is a target protein of mir-338-3p and is associated with poor prognosis and progression of renal cell carcinoma. *Oncol Res*. 2018; **27**: 125-37.

12. Cosenza MR, Krämer A. Centrosome amplification, chromosomal instability and cancer: mechanistic, clinical and therapeutic issues. *Chromosome Res*. 2016; **24**: 105-26.

13. Imai T, Oue N, Yamamoto Y, et al. Overexpression of KIFC1 and its association with spheroid formation in esophageal squamous cell carcinoma. *Pathol Res Pract*. 2017; **213**: 1388-93.

14. Sekino Y, Oue N, Shigematsu Y, et al. KIFC1 induces resistance to docetaxel and is associated with survival of patients with prostate cancer. *Urol Oncol Semin Orig Investig*. 2017; **35**: 31.e13-31.e20.

15. Yukawa M, Yamauchi T, Kurisawa N, Ahmed S, Kimura K, Toda T. Fission yeast cells overproducing HSET/KIFC1 provides a useful tool for identification

and evaluation of human kinesin-14 inhibitors. *Fungal Genet Biol*. 2018; **116**: 33-41.

16. Kurisawa N, Yukawa M, Koshino H, Onodera T, Toda T, Kimura K. Kolavenic acid analog restores growth in HSET-overproducing fission yeast cells and multipolar mitosis in MDA-MB-231 human cells. *Bioorganic Med Chem*. 2020; **28**: 115154.

17. Kondo T, Oue N, Yoshida K, et al. Expression of POT1 is Associated with Tumor Stage and Telomere Length in Gastric Carcinoma. *Cancer Res*. 2004; **64**: 523-9 LP-529.

18. Ying H, Xu Z, Chen M, Zhou S, Liang X, Cai X. Overexpression of Zwint predicts poor prognosis and promotes the proliferation of hepatocellular carcinoma by regulating cell-cycle-related proteins. *Onco Targets Ther*. 2018; **11**: 689-702.

19. Yasui W, Ayhan A, Kitadai Y, et al. Increased expression of p34cdc2 and its kinase activity in human gastric and colonic carcinomas. *Int J Cancer*. 1993; **53**: 36-41.

20. Sakamoto N, Oue N, Sentani K, et al. Liver-intestine cadherin induction by epidermal growth factor receptor is associated with intestinal differentiation of gastric cancer. *Cancer Sci*. 2012; **103**: 1744-50.

21. Fujita T, Chiwaki F, Takahashi RU, et al. Identification and characterization of CXCR4-positive gastric cancer stem cells. *PLoS One*. 2015; **10**: 1-19.

22. Li S, Schmitz KR, Jeffrey PD, Wiltzius JJW, Kussie P, Ferguson KM. Structural basis for inhibition of the epidermal growth factor receptor by cetuximab. *Cancer Cell*. 2005; **7**: 301-11.

23. Fang JY RB. The MAPK signalling pathways and colorectal cancer. *Lancet Oncol*. 2005; **6**: 322-27.

24. Cimino SK, Eng C. Up-and-coming experimental drug options for metastatic colorectal cancer. *J Exp Pharmacol*. 2020; **12**: 475-85.

25. Grothey A, Sobrero AF, Shields AF, et al. Duration of adjuvant chemotherapy for stage III colon cancer. *N Engl J Med*. 2018; **378**: 1177-88.

26. Kim N, Song K. KIFC1 Is Essential for Bipolar Spindle Formation and Genomic Stability in the Primary Human Fibroblast IMR-90 Cell. *Cell Struct Funct*. 2013; **38**: 21-30.

27. Xiao Y-X, Yang W-X. KIFC1: a promising chemotherapy target for cancer treatment? *Oncotarget*. 2016; **7**: 48656-70

28. Wang H, Hu X, Ding X, et al. Human Zwint-1 specifies localization of Zeste White 10 to kinetochores and is essential for mitotic checkpoint signaling. *J Biol Chem*. 2004; **279**: 54590-8.

29. Lin YT, Chen Y, Wu G, Lee WH. Hec1 sequentially recruits Zwint-1 and ZW10 to kinetochores for faithful chromosome segregation and spindle checkpoint control. *Oncogene*. 2006; **25**: 6901-14.

30. Yuan W, Xie S, Wang M, et al. Bioinformatic analysis of prognostic value of ZW10 interacting protein in lung cancer. *Onco Targets Ther*. 2018; **11**: 1683-95.

31. Todaro M, Francipane MG, Medema JP, Stassi G. Colon Cancer Stem Cells: Promise of Targeted Therapy. *Gastroenterology*. 2010; **138**: 2151-62.

32. Clarke MF, Al-Hajj M, Morrison SJ, Wicha MS, Benito-Hernandez A. Prospective identification of tumorigenic breast cancer cells. *Proc Natl Acad Sci*. 2003; **100**: 3983-88.

33. Pan S, Zhan Y, Chen X, Wu B, Liu B. Identification of Biomarkers for Controlling Cancer Stem Cell Characteristics in Bladder Cancer by Network Analysis of Transcriptome Data Stemness Indices. *Front Oncol*. 2019; **9**: 1-11.

34. Liu D, Xu X, Wen J, et al. Integrated Genome-Wide Analysis of Gene Expression and DNA Copy Number Variations Highlights Stem Cell-Related Pathways in Small Cell Esophageal Carcinoma. *Stem Cells Int*. 2018; **2018**: 1-9.

Figure legends

Figure 1 Expression of KIFC1 in CRC tissue samples. (a) qRT-PCR analysis of *KIFC1* in 14 kinds of normal tissues and 28 CRC tissue samples. The units are arbitrary, and *KIFC1* expression was standardized against 1.0 μg of total RNA from normal colon tissue as 1.0. (b) Immunohistochemical staining of KIFC1 in colon adenocarcinoma. Left panel, original magnification, ×40. Right panel, a high-magnification image of the field designated by a box in the left panel. Original magnification, ×400. (c) Immunohistochemical analysis of KIFC1, CD44, and ALDH1. Original magnification, ×100. Right-upper panel, a high-magnification image of the field designated by a black box. Original magnification, ×400. (d) Kaplan–Meier plot of overall survival of CRC patients. (e) Kaplan–Meier plot of short-term survival (1 to 80 months) of CRC patients in TCGA database.

Figure 2 Functional analysis of KIFC1 in CRC cells. (a) Western blot analysis of KIFC1 in 4 CRC cell lines. (b) Western blot analysis of KIFC1, Akt, phospho-Akt (pAkt), Erk 1/2 and phospho-Erk1/2 (pErk1/2) in lysates of DLD-1 and WiDr cells transfected with KIFC1 siRNA or negative control siRNA. β-actin was used as a loading control. (c) Effects of *KIFC1* knockdown on DLD-1 and WiDr cell growth. Cell growth was assessed spectrometrically by MTT assay at 1, 2, and 4 days after seeding. Bars and error bars indicate mean and S.D., respectively, of three independent experiments. (d) Number and size of spheroids formed by DLD-1 and WiDr cells

transfected with KIFC1 or negative control siRNAs. Bars and error bars indicate mean and S.D., respectively, of three independent experiments.

Figure 3 Cytotoxic effect of KIFC1 inhibitor and analysis of ZWINT expression. (a) KAA inhibited CRC growth in a dose-dependent manner. Cell growth was assessed spectrometrically by MTT assay at 1, 2, and 4 days after seeding. Bars and error bars indicate mean and S.D., respectively, of three independent experiments. NS, not significant. (b) Immunohistochemical staining of KIFC1 and ZWINT in colon adenocarcinoma. Original magnification, ×40. Right-lower panel, a high-magnification image of the field designated by a black box. Original magnification, ×400. (c) Kaplan–Meier plot of overall survival of CRC patients. (d) Correlation between *KIFC1* and *ZWINT* expressions in colorectal adenocarcinoma samples in TCGA gene-level expression data (n = 512). (e) KIFC1 and ZWINT expressions reduced by KIFC1 inhibitor in a time-dependent manner. (f) ZWINT expression downregulated in KIFC1 siRNA-transfected cells. β-actin was used as a loading control.

Figure 4 Effect of ZWINT inhibition on the biological functions of CRC cells. (a) Western blot analysis of ZWINT, KIFC1, Akt, pAkt, Erk1/2, and pErk1/2 in lysates of CRC cells transfected with ZWINT siRNA or negative control siRNA. β-actin was used as a loading control. (b) *ZWINT* knockdown inhibited CRC cell growth. Cell growth was assessed spectrometrically by MTT assay at 1, 2, and 4 days after seeding. Bars and

error bars indicate mean and S.D., respectively, of three independent experiments. (c) Number and size of spheroids formed by CRC cells transfected with ZWINT or negative control siRNA. Bars and error bars indicate mean and S.D., respectively, of three independent experiments.

List of supplementary material

Supplementary Material and methods Quantitative reverse transcription PCR (qRT-PCR), Western blot, Gene expression data from The Cancer Genome Atlas (TCGA), Wound healing assay**,** Conventional adenoma tissue samples

Supporting Table 1 Primer sequences used for qRT-PCR

Supporting Table 2 Clinicopathologic characteristics of 28 patients with CRC

Supporting Table 3 List of genes downregulated by the KIFC1-specific inhibitor, kolavenic acid analog

Supporting Table 4 Correlation between ZWINT expression and clinicopathologic characteristics

Supporting Figure 1 Representative images and wound contraction percentage of a wound-healing assay in DLD-1 (a) and WiDr (b) cells treated with KAA. Bars and error bars indicate mean and S.D., respectively, of three independent experiments. NS, not significant.

Supporting Figure 2 Comparison of mRNA expression levels of genes downregulated by the KIFC1 inhibitor (kolavenic acid analog) in CRC tissue samples. Fold changes between CRC tissue (T) and corresponding non-neoplastic mucosa (N) are demonstrated.

Supporting Figure 3 Summary of immunohistochemical staining of KIFC1 and ZWINT in conventional colon adenomas. The graph indicates the number of cases with staining status. CALG, conventional adenoma low grade; CAHG, conventional adenoma high grade.

Fig. 1

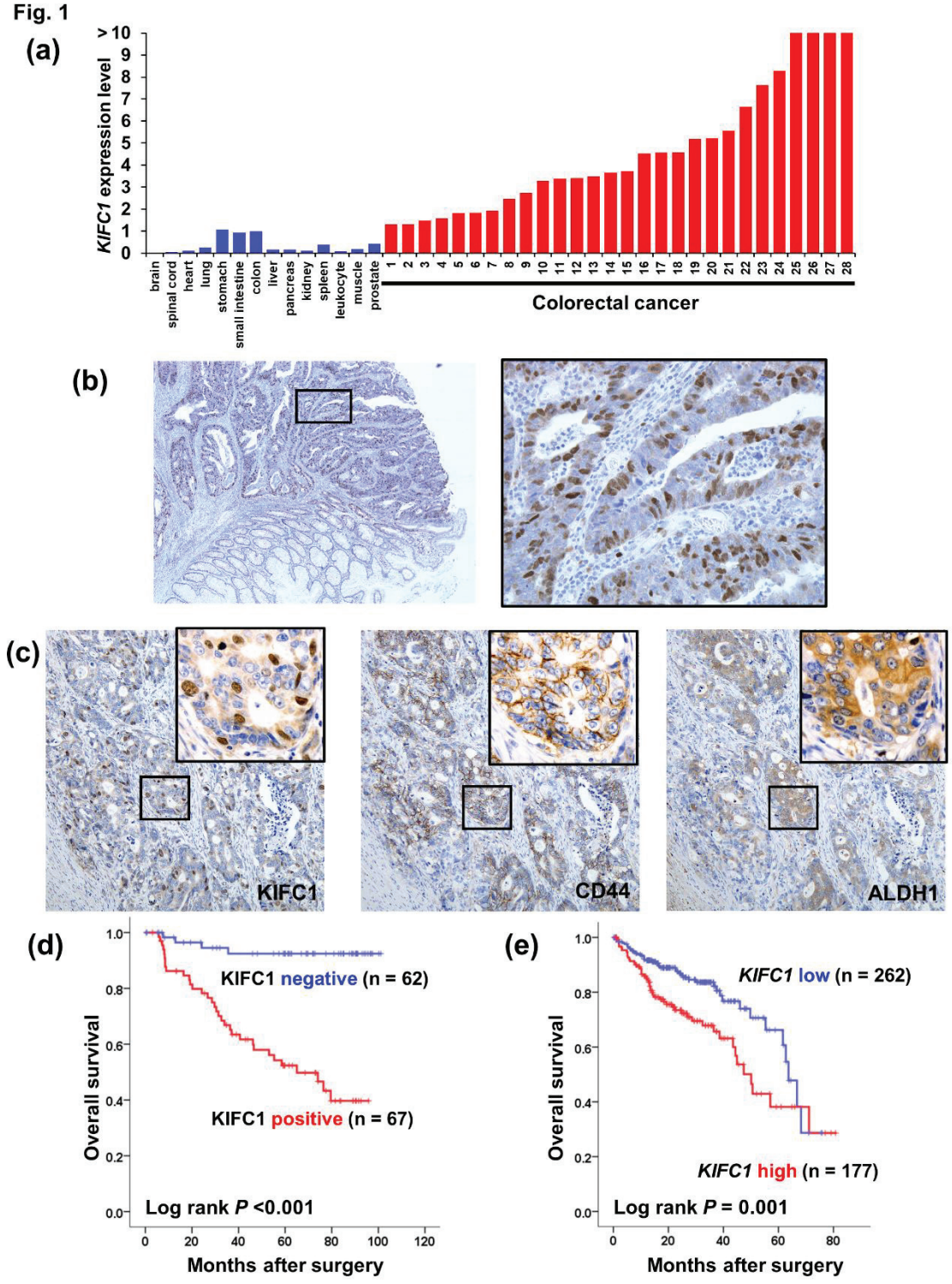
(a)
KIFC1 expression level
> 10
9
8
7
6
5
4
3
2
1
0
brain
spinal cord
heart
lung
stomach
small intestine
colon
liver
pancreas
kidney
spleen
leukocyte
muscle
prostate
1 2 3 4 5 6 7 8 9 10 11 12 13 14 15 16 17 18 19 20 21 22 23 24 25 26 27 28
Colorectal cancer
(b)
(c)
KIFC1
CD44
ALDH1
(d)
KIFC1 negative (n = 62)
KIFC1 positive (n = 67)
Overall survival
1.0
0.8
0.6
0.4
0.2
0.0
Log rank P <0.001
0 20 40 60 80 100 120
Months after surgery
(e)
KIFC1 low (n = 262)
KIFC1 high (n = 177)
Overall survival
1.0
0.8
0.6
0.4
0.2
0.0
Log rank P = 0.001
0 20 40 60 80
Months after surgery

Fig. 2

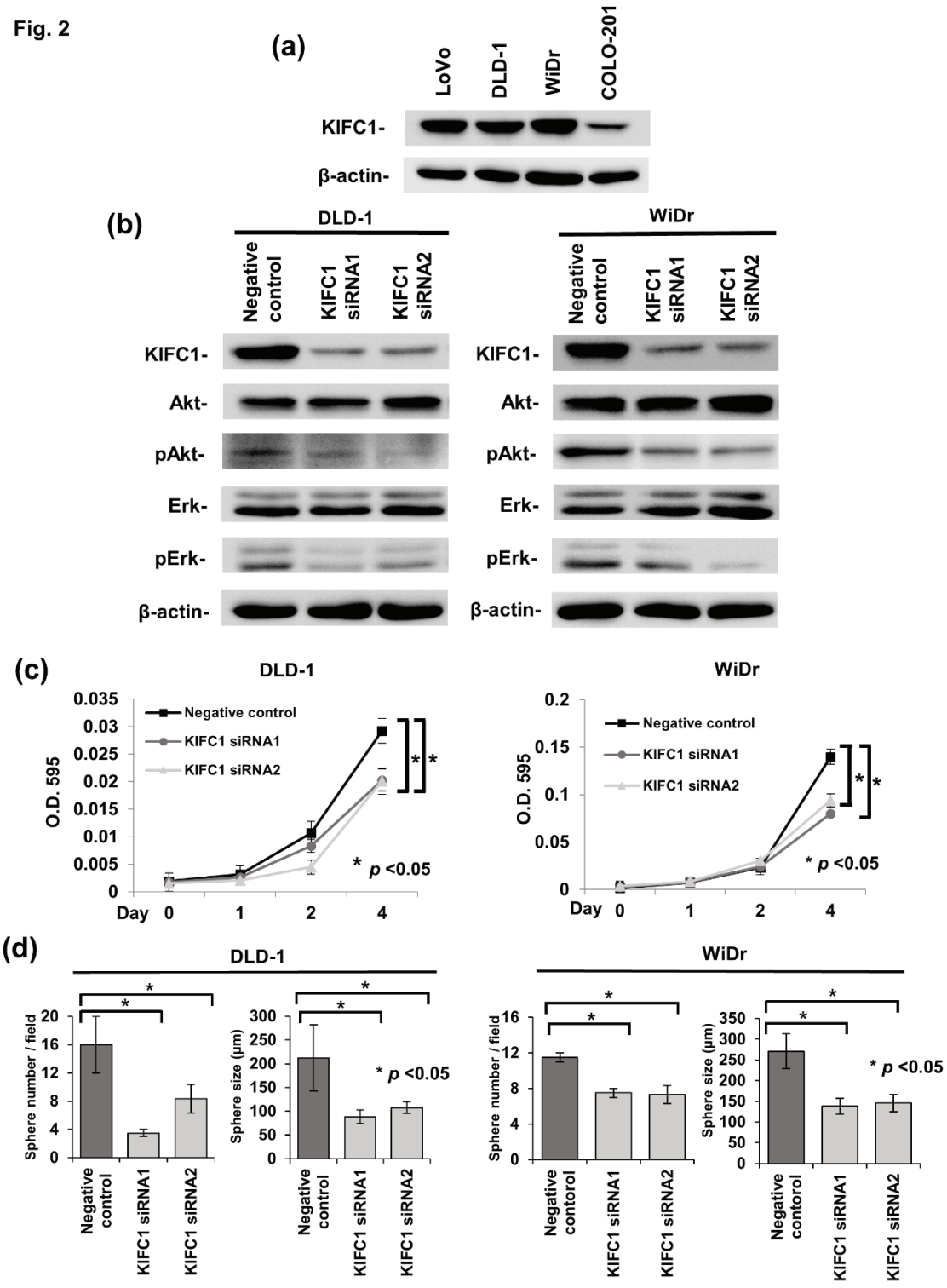
(a)
LoVo
DLD-1
WiDr
COLO-201
KIFC1-
β-actin-
(b)
DLD-1
WiDr
Negative control
KIFC1 siRNA1
KIFC1 siRNA2
KIFC1-
Akt-
pAkt-
Erk-
pErk-
β-actin-
(c)
DLD-1
WiDr
Negative control
KIFC1 siRNA1
KIFC1 siRNA2
O.D. 595
Day 0 1 2 4
* p <0.05
(d)
DLD-1
WiDr
Sphere number / field
Sphere size (μm)
Negative control
KIFC1 siRNA1
KIFC1 siRNA2
* p <0.05

Fig. 3

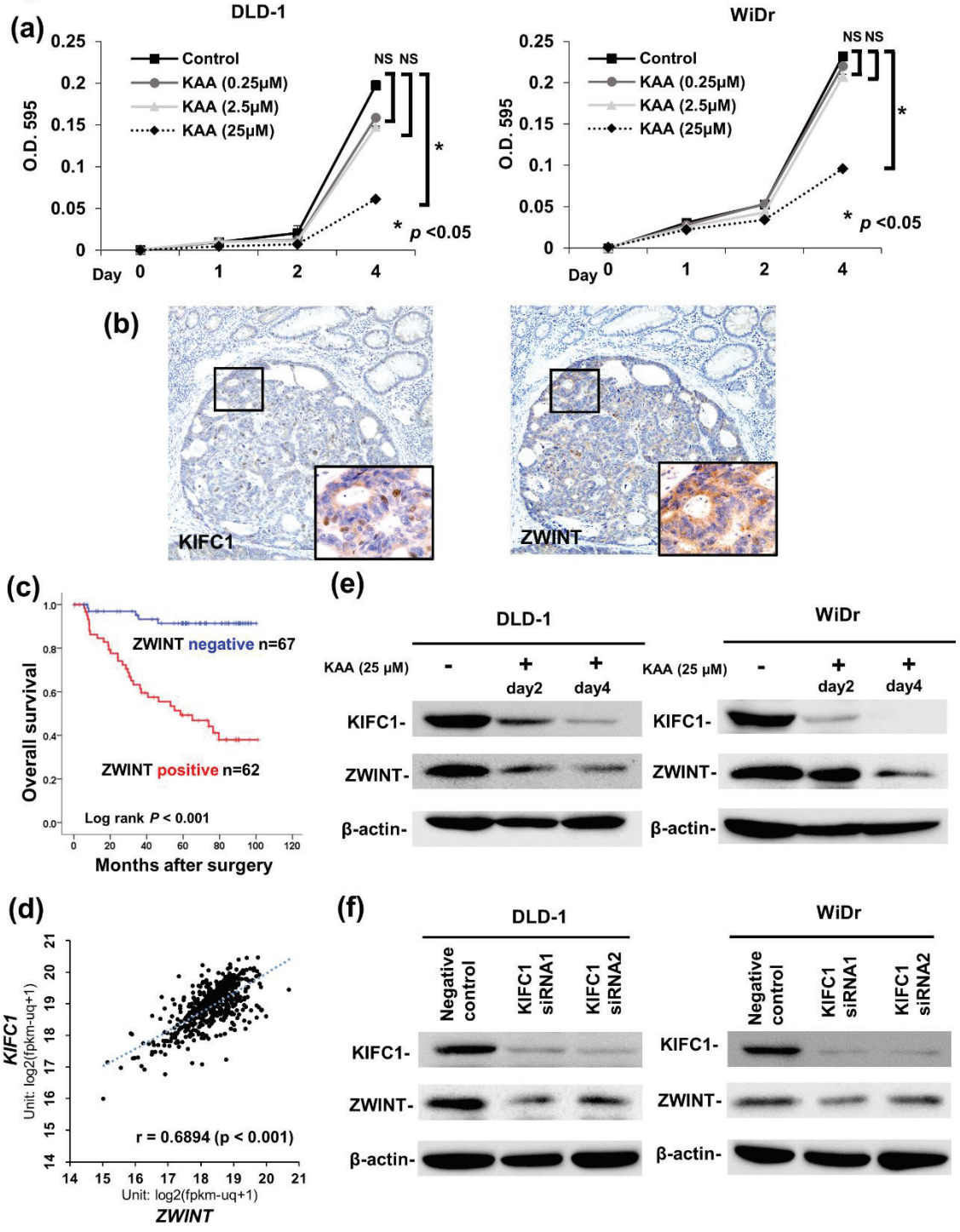
(a)
DLD-1
WiDr
Control
KAA (0.25μM)
KAA (2.5μM)
KAA (25μM)
O.D. 595
Day
NS NS
*
p <0.05
(b)
KIFC1
ZWINT
(c)
Overall survival
ZWINT negative n=67
ZWINT positive n=62
Log rank P < 0.001
Months after surgery
(d)
KIFC1
ZWINT
Unit: log2(fpkm-uq+1)
r = 0.6894 (p < 0.001)
(e)
DLD-1
WiDr
KAA (25 μM)
day2
day4
KIFC1-
ZWINT-
β-actin-
(f)
DLD-1
WiDr
Negative control
KIFC1 siRNA1
KIFC1 siRNA2
KIFC1-
ZWINT-
β-actin-

Fig. 4

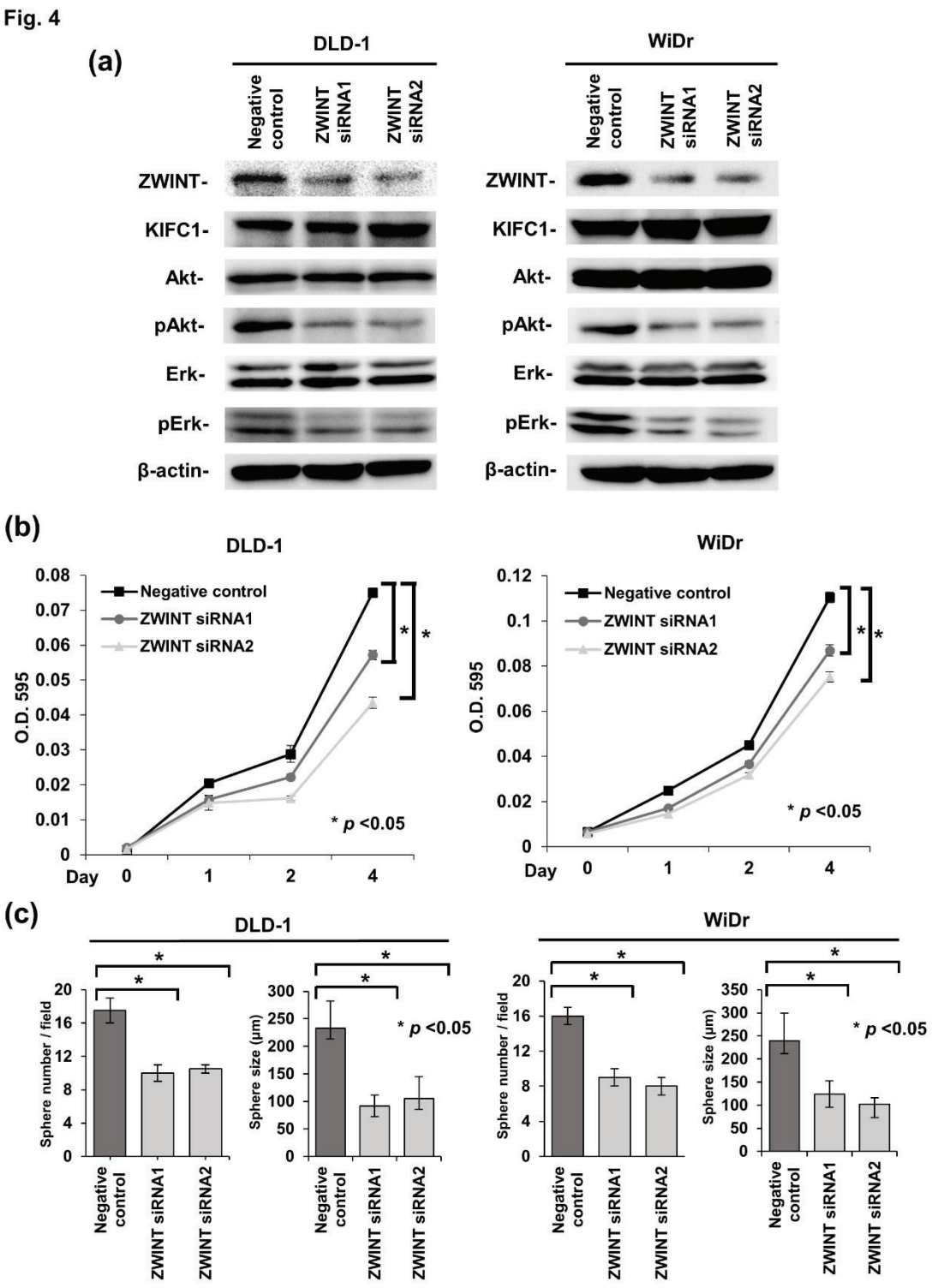
(a)
DLD-1
WiDr
Negative control
ZWINT siRNA1
ZWINT siRNA2
ZWINT-
KIFC1-
Akt-
pAkt-
Erk-
pErk-
β-actin-
(b)
DLD-1
WiDr
Negative control
ZWINT siRNA1
ZWINT siRNA2
O.D. 595
Day
* p <0.05
(c)
DLD-1
WiDr
Sphere number / field
Sphere size (μm)
* p <0.05

Table 1 Correlation between KIFC1 expression and cancer stem cell markers

	KIFC1 expression		*p*-value*
	Positive	**Negative**	
CD44			**0.011**
Positive	**41 (63 %)**	**24**	
Negative	**26 (41 %)**	**38**	
ALDH1			**0.009**
Positive	**37 (65 %)**	**20**	
Negative	**30 (42 %)**	**42**	

* **Chi-square test**

Table 2 Relationship between KIFC1 expression and clinicopathologic characteristics

	KIFC1 expression		*p*-value*
	Positive	Negative	
Age			**0.115**
≤ 60	**26 (62 %)**	**16**	
> 60	**41 (47 %)**	**46**	
Sex			**0.487**
Men	**22 (48 %)**	**24**	
Women	**45 (54 %)**	**38**	
Tumor location			**0.502**
Right colon	**18 (47 %)**	**20**	
Left colon	**49 (54 %)**	**42**	
Histological classification			**0.822**
Well/moderate	**62 (52 %)**	**58**	
Poor/mucinous	**5 (56 %)**	**4**	
T classification			**0.104**
T1/T2	**17 (42 %)**	**24**	
T3/T4	**50 (57 %)**	**38**	
N classification			**0.011**
N0	**25 (40 %)**	**37**	
N1/N2/N3	**42 (63 %)**	**25**	
M classification			**< 0.001**
M0	**44 (44 %)**	**57**	
M1	**23 (82 %)**	**5**	
Stage			**0.001**
Stage I/II	**21 (36 %)**	**37**	
Stage III/IV	**46 (65 %)**	**25**	
ZWINT expression			**< 0.001**
Negative	**20 (29 %)**	**48**	
Positive	**47 (77 %)**	**14**	

* **Chi-square test**

Table 3 Univariate and multivariate Cox regression analysis of overall survival

	Univariate analysis			Multivariate analysis		
	HR	**95 % CI**	***p*-value**	**HR**	**95 % CI**	***p*-value**
Age			**0.870**			
≤60	**1 (Ref.)**					
>60	**0.946**	**0.486–1.840**				
Sex			**0.427**			
Men	**1 (Ref.)**					
Women	**0.756**	**0.380–1.506**				
Tumor location			**0.100**			
Right colon	**1 (Ref.)**					
Left colon	**0.572**	**0.294–1.113**				
Histological classification			**0.058**			
Well/moderate	**1 (Ref.)**					
Poor/mucinous	**2.73**	**0.965–7.721**				
Stage			**< 0.001**			**0.002**
Stage I/II	**1 (Ref.)**			**1 (Ref.)**		
Stage III/IV	**12.617**	**3.867–41.170**		**6.997**	**2.083–23.508**	
KIFC1 expression			**< 0.001**			**0.029**
Negative	**1 (Ref.)**			**1 (Ref.)**		
Positive	**9.318**	**3.293–26.369**		**3.642**	**1.142–11.609**	
ZWINT expression			**< 0.001**			**0.035**
Negative	**1 (Ref.)**			**1 (Ref.)**		
Positive	**8.912**	**3.468–22.906**		**3.139**	**1.087–9.068**	

HR, hazard ratio; CI, confidence interval

Supplementary Material and methods

Quantitative reverse transcription PCR (qRT-PCR)

Total RNA was extracted using RNeasy Mini Kit (Qiagen, Valencia, CA, USA) and 1 μg of total RNA was converted to cDNA with First Strand cDNA Synthesis Kit (Amersham Biosciences Corp., Piscataway, NJ, USA). qPCR was performed using SYBR Green PCR Core Reagents Kit (Applied Biosystems, Foster City, CA, USA) and the emission intensity was detected on ABI PRISM 7700 Sequence Detection System (Applied Biosystems) as described previously.[17] β-actin (*ACTB* gene)-specific PCR products amplified from the same RNA samples served as internal control. Primer sequences used in this analysis are summarized in Supporting Table 1.

Western blot

Cells were lysed as previously described.[19] The lysates (40 μg) were solubilized in Laemmli sample buffer by boiling and then subjected to 10 % SDS-PAGE. Following electrophoresis, the bands were electrotransferred onto a nitrocellulose membrane that was further incubated with primary antibodies against KIFC1 and ZWINT. Peroxidase-conjugated anti-mouse and anti-rabbit IgG were used in the secondary reaction. Immunocomplexes were visualized with ECL Western Blot Detection system (Amersham Biosciences Corp.). β-actin (Sigma, St. Louis, MO, USA) was used as the loading control.

Gene expression data from The Cancer Genome Atlas (TCGA)

For analyzing gene expression data, TCGA colon adenocarcinoma gene-level expression data (n = 439 samples, version 2016) were downloaded from OncoLnc (*http://www.oncolnc.org/*). In the Kaplan–Meier analysis, we used receiver operating characteristic (ROC) curve analysis to define the cut-off point for the KIFC1 expression that correlated with the prognosis. *KIFC1* expression was considered high if the expression score was above the cut-off value and low if the score was equal to or below the cut-off value. For analyzing the correlation between *KIFC1* and *ZWINT* expressions, TCGA colon adenocarcinoma gene-level expression data (n = 512 samples, version 2019) were downloaded from UCSC Xena hub (*http://xena.ucsc.edu*) as $\log_2$ values of the RSEM normalized counts.

Wound healing assay

To carry out the wound healing assay, the treated cells were plated onto collagen‐coated coverslips. The monolayer cells were then scratched manually with a plastic pipette tip, and after being washed with PBS, the wounded monolayers of the cells were allowed to heal in RPMI 1640 containing 10% FBS. Wound healing was measured by wound contraction percentage and captured at 0, 24, 48, or 60 hours after scratching.

Conventional adenoma tissue samples

Twenty primary colorectal adenoma samples were collected from patients who underwent endoscopic or surgical resection at Hiroshima University Hospital or its affiliated hospitals. The distribution of colorectal adenomas was as follows: conventional adenoma low grade (CALG), n = 10; conventional adenoma high grade (CAHG), n = 10.

Supporting Table 1 Primer sequences used for qRT-PCR

Gene	Forward primer	Reverse primer
KIFC1	GACGCCCTGCTTCATCTG	CCAGGTCCACAAGACTGAGG
FAM111B	TGGACAGACTCTCCGGTTCT	TCTGCTTCATGACAGTATCCTTG
CEP128	GGATCTCTGCAGGACCGTGTA	TTCTCAGGCACAGACTCCAGA
METTL7A	GCATTGCAGAGAACCGACAC	AAATAGAAAGCCCCTCCCGGT
ARHGEF39	GTCTCCTCAAGGTGACAGCC	AACCACCGTCAATGAGCACT
ERN2	TGCTCATTGGACACCACGAG	CGGCTGTTGCTCCAAGAAGA
ACSM3	GGTTCAGGGCTGCTCTTCTA	CGCTGAAAACACTTGGCATGA
ZWINT	AGGTTTCTGCAGAGGGTAAGC	ACAGCCTTGAAGGACACACC

Supporting Table 2 Clinicopathologic characteristics of 28 patients with CRC

Number of cases	28
Age, median (range)	68 (43-93)
Sex (%)	
Men	14 (50%)
Women	14 (50%)
Tumor location (%)	
Right colon	16 (57%)
Left colon	12 (43%)
Differentiation (%)	
Well/moderate	22 (79%)
Poor/mucinous	6 (21%)
pT classification (%)	
T1/T2	9 (32%)
T3/T4	19 (68%)
pN classification (%)	
N0	13 (46%)
N1/N2/N3	15 (54%)
pM classification (%)	
M0	25 (89%)
M1	3 (11%)
pStage (%)	
Stage I/II	13 (46%)
Stage III/IV	15 (54%)

Supporting Table 3 List of genes downregulated by the KIFC1 inhibitor, kolavenic acid analog

Gene symbol	Gene name	Fold change
FAM111B	family with sequence similarity 111, member B	0.137738139
CEP128	centrosomal protein 128 kDa	0.153893052
METTL7A	methyltransferase like 7A	0.156041319
ARHGEF39	Rho guanine nucleotide exchange factor 39	0.167240944
ERN2	endoplasmic reticulum to nucleus signaling 2	0.211686328
ACSM3	acyl-CoA synthetase medium-chain family member 3	0.251738888
ZWINT	ZW10 interacting kinetochore protein	0.267943366
KIFC1	kinesin family member C1	0.332171454

Supporting Table 4 Correlation between ZWINT expression and clinicopathologic characteristics

	ZWINT expression		*p*-value*
	Positive	Negative	
Age			0.421
≤ 60	22 (52 %)	20	
> 60	39 (45 %)	48	
Sex			0.080
Men	44 (53 %)	39	
Women	17 (37 %)	29	
Tumor location			0.432
Right colon	20 (53 %)	18	
Left colon	41 (45.1 %)	50	
Histological classification			0.227
Well/moderate	55 (46 %)	65	
Poor/mucinous	6 (67 %)	3	
pT classification			< 0.001
T1/T2	10 (24 %)	31	
T3/T4	51 (58 %)	37	
pN classification			< 0.001
N0	17 (27 %)	45	
N1/N2/N3	44 (66 %)	23	
pM classification			0.001
M0	40 (40 %)	61	
M1	21 (75 %)	7	
pStage			<0.001
Stage I/II	15 (26 %)	43	
Stage III/IV	46 (65 %)	25	

* Chi-square test

(a)

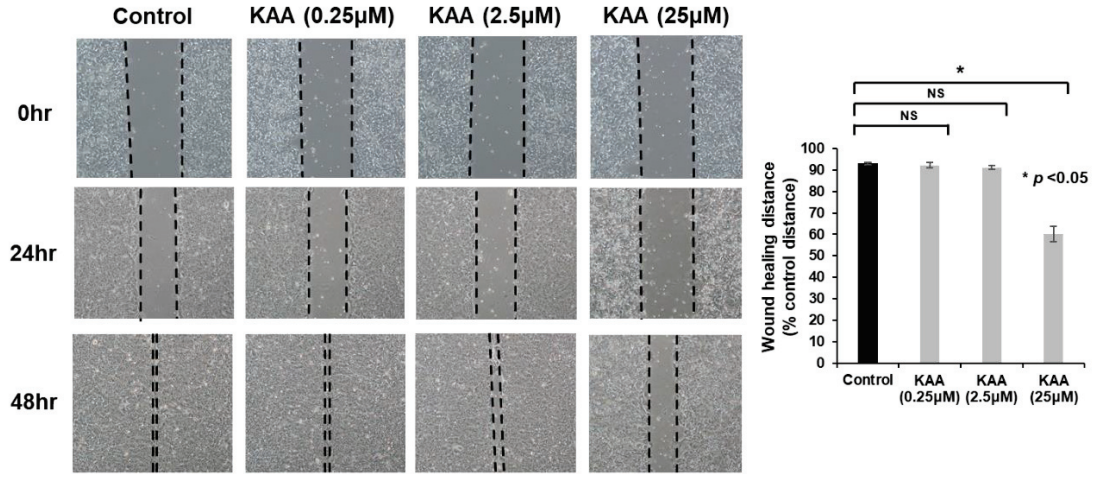

(b)

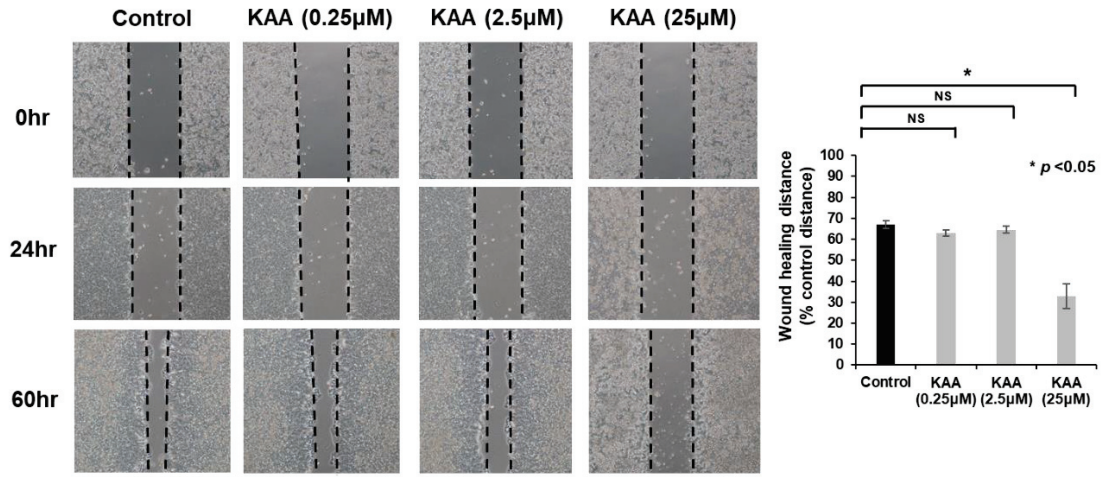

Supporting Figure 1 Representative images and wound contraction percentage of a wound-healing assay in DLD-1 (a) and WiDr (b) cells treated with KAA. Bars and error bars indicate mean and S.D., respectively, of three independent experiments. NS, not significant.

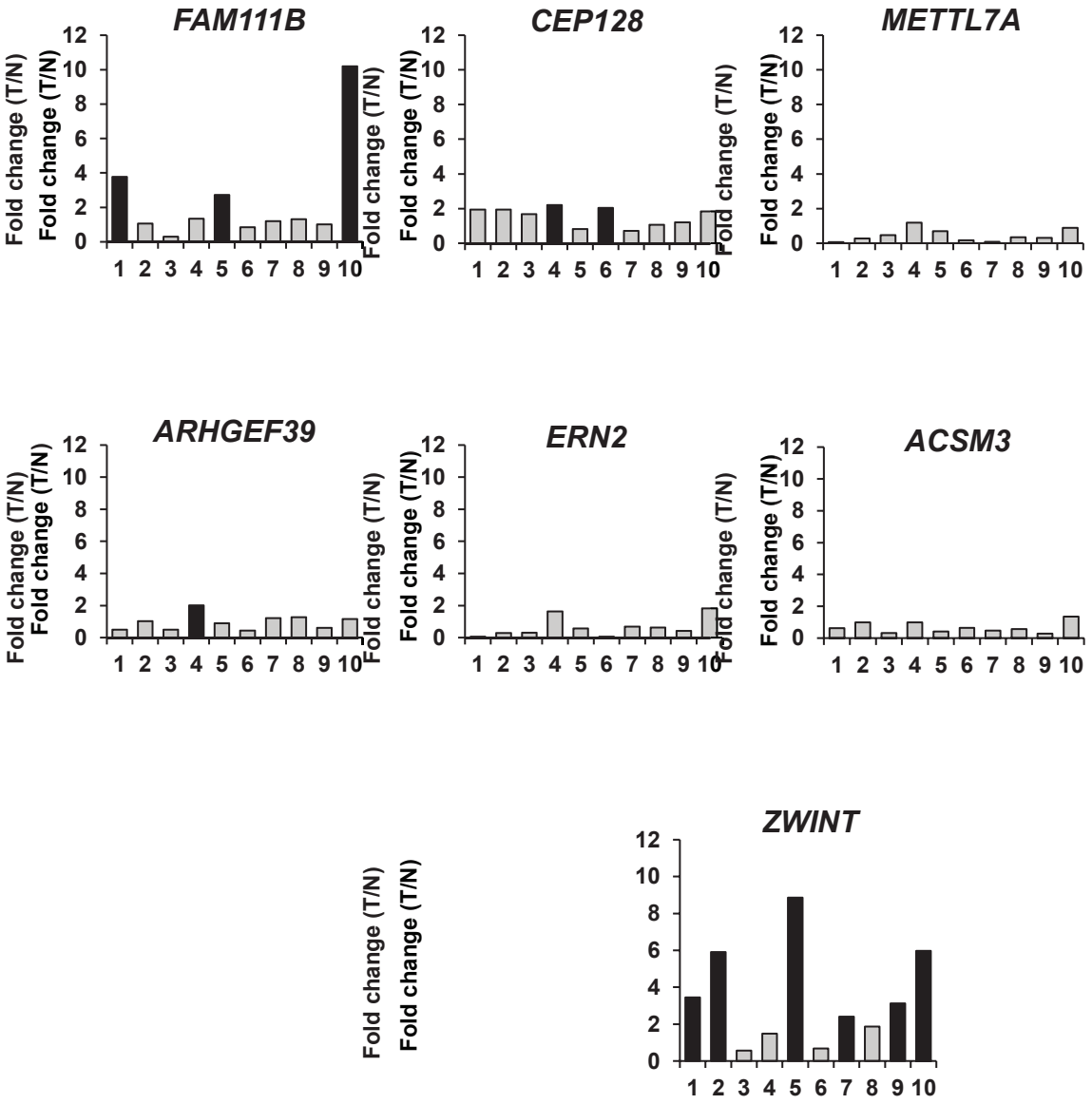

Supporting Figure 2 Comparison of mRNA expression levels of genes downregulated by the KIFC1 inhibitor (kolavenic acid analog) in CRC tissue samples. Fold changes between CRC tissue (T) and corresponding non-neoplastic mucosa (N) are demonstrated.

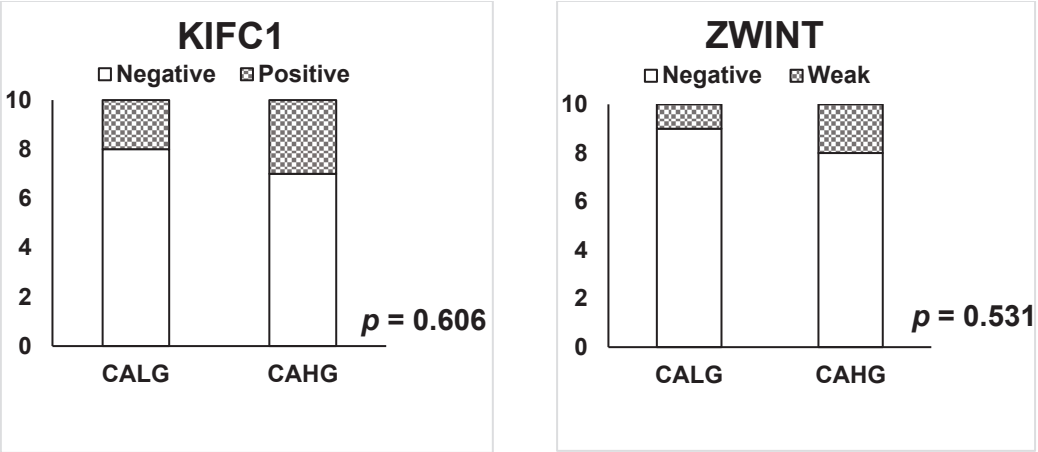

Supporting Figure 3 Summary of immunohistochemical staining of KIFC1 and ZWINT in conventional colon adenomas. The graph indicates the number of cases with staining status. CALG, conventional adenoma low grade; CAHG, conventional adenoma high grade.